Nuclear Physics A400 (1983) 63c-94c.

PROSPECTS OF INTERMEDIATE ENERGY NUCLEAR COLLISIONS

Horst STÖCKER

National Superconducting Cyclotron Laboratory and
Department of Physics and Astronomy
Michigan State University, East Lansing, MI 48824-1321

and

G. BUCHWALD, G. GRAEBNER, P. SUBRAMANIAN*,
J.A. MARUHN and W. GREINER

Institut für Theoretische Physik, J.W. Goethe-Universität
D-6000 Frankfurt am Main, Germany

and

B.V. JACAK and G.D. WESTFALL

National Superconducting Cyclotron Laboratory
Michigan State University, East Lansing, MI 48824-1321

Abstract: We focus on central nuclear collisions--"multifragmentation events"--in the energy range 20-400 MeV/n. They seem well suited to study bulk properties of nuclear matter at moderate entropies. Various ways of extracting information on the produced entropy are discussed. We emphasize the importance of medium mass fragment production for this goal. The consequences of a first order liquid-vapor phase transition at low densities $\rho<\rho_0$ are pointed out--the release of latent heat results in an increase of the entropy at energies $E_{LAB} \lesssim 200$ MeV/n. It is pointed out that a minimum in the mass distribution is indicative of the onset of condensation. Such a minimum has indeed been observed in multifragmentation events. The medium energy reactions also provide an enhanced sensitivity to the stiffness of the nuclear equation of state at high densities $\rho>\rho_0$. This is discovered in a 4π exclusive energy flow analysis performed on the basis of the nuclear fluid dynamical model. A strong bombarding energy dependence of the flow effects is predicted, which is not found in cascade simulations. The flow analysis can also be used to reveal the presence of a high density abnormal state via a characteristic change of the flow pattern at a critical bombarding energy.

The availability of the 84 MeV/n ^{12}C-beam at CERN and heavier beams at LBL have only recently enabled first exploratory experiments[1-14]) on nuclear collisions at intermediate energies. One of the most challenging motivations for doing these experiments is the opportunity to study nuclear matter at other than ground state densities and at moderate temperatures and entropies[6,15-18]). Over this medium energy regime, we expect a transition from the mean field phenomena typical of low energy reactions to two (and more) nucleon collisions for high energy reactions[6,15-18]). Fig. 1 shows the reaction dynamics as predicted by a quantal, mean field TDHF calculation[16]) compared to the semiclassical, macroscopic nuclear fluid dynamical model[15,16]). The latter assumes that the incident nucleons

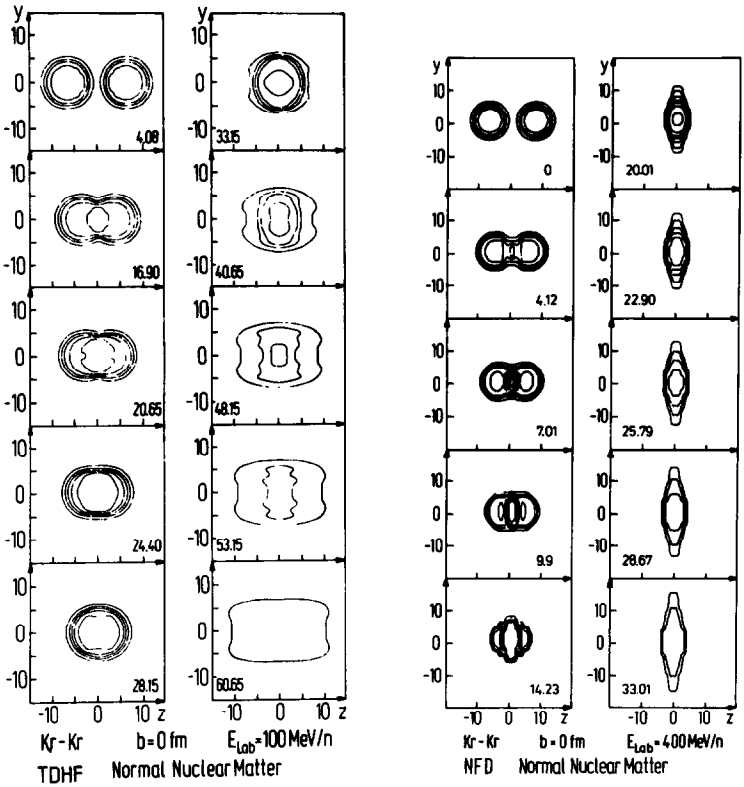

Fig. 1

have a short mean free path; therefore the nuclei stop each other and the matter is squeezed to the side. The TDHF model, on the other hand, neglects nucleon-nucleon collisions, i.e. the nuclei are more transparent to each other, and hence the nucleons show forward-backward peaked emission patterns (left)[16].

1. Information on the produced entropy from light and medium mass fragments

In spite of the differences in the emission pattern, a consistent picture emerges from these calculations, as well as from intranuclear cascade calculations[19-21] for the evolution of the density and temperature of the system (see fig. 2). As the nuclei interpenetrate each other, nuclear matter is compressed and highly excited. From the state of highest density ($\rho \gtrsim 2\text{-}4\ \rho_0$) and temperature T, the system expands at approximately constant entropy towards lower densities, $\rho \lesssim \rho_0/2$. During the expansion the temperature drops as shown in fig. 2. In the late stages of the reaction the system disintegrates and the finally observed fragments are formed[22-28]. Hence, it has to be pointed out that the temperature values derived from the experimentally observed slope factors[24], shown in fig. 3, do not reflect the actual initial temperature directly. However, the matter picks up a collective kinetic flow

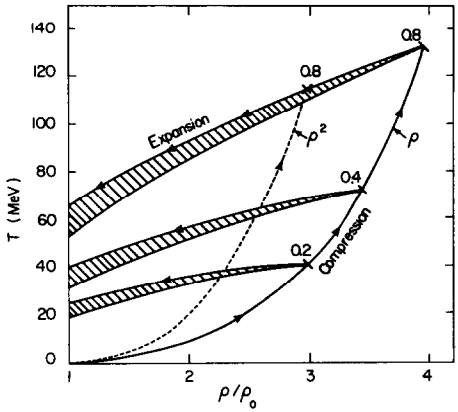

Fig. 2

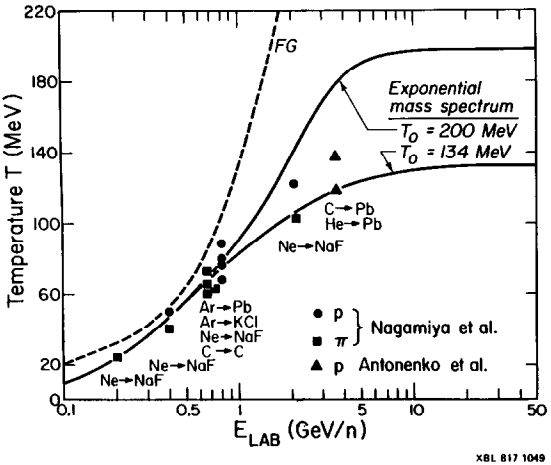

Fig. 3

energy even though the random thermal kinetic energy of the particles drops, so the finally observed slopes of the spectra do not deviate too much from the initial temperature value, as can be seen in fig. 3[26]). A state variable which does stay constant during the expansion is the entropy per nucleon, S/A. Hence, it is of great importance to find a measure for the entropy, since this can yield insight on the properties of the system at high densities and temperatures. It was suggested[23]) that entropy can be deduced from the observed proton-to-deuteron ratio R_{dp}: in chemical equilibrium, the entropy is determined as

$$S/A = 3.95 - \ell n\ R_{dp} \qquad (1)$$

if the number of protons in the equilibrium greatly exceeds the number of deuterons $\langle p\rangle_{equilibrium} >> \langle d\rangle_{equilibrium}$, and if other clusters can be neglected[23]). This seems to be promising, since it has been shown[22]) that chemical equilibrium can indeed be established towards the late states of the expansion, so that the law of mass action can be applied. Since experimentally $R_{tp} << R_{dp} \lesssim 0.4$ at

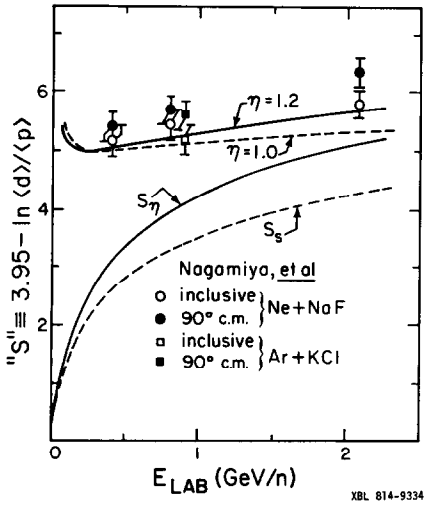

Fig. 4

$E_{LAB} \gtrsim 400$ MeV/n[24]), the other conditions for this simple formula to be valid seem to be fulfilled as well. However, the entropy extracted from the data[24]) is much larger than expected[23]).

Figure 4 shows the entropy as obtained from a hydrodynamical calculation[25]) compared with the data. The experimental values of "S" exceed the calculated values, in particular for $E_{LAB} \leq 400$ MeV/n. On the other hand, the proton-to-deuteron ratios obtained from the hydrodynamical model combined with a chemical equilibrium calculation[25]), agree well with the experimental data over the whole range of bombarding energies considered. This apparent paradox is explained by the subsequent decay of particle unstable excited nuclei, $A^* \rightarrow (A-1) + p$, which becomes increasingly important at intermediate and low energies[25,29]). Hence the relation between the entropy, S, and the observed R_{dp} is not given by the simple formula (eq. (1)). To study this question further, we have extended the current quantum statistical models[27,28]) to take into account simultaneously particle unstable nuclides and ground state nuclei up to mass 25, as well as Bose condensation of the integer spin nuclides, excluded volume effects, pions and the delta resonance[29]).

Baryon number and charge conservation are achieved via

$$\overline{Z} = \sum_{i=1}^{N} n_i(Z_i,N_i)\cdot Z_i \qquad (2)$$

$$\overline{N} = \sum_{i=1}^{N} n_i(Z_i.N_i)\cdot N_i \qquad (3)$$

where n_i is the number of particles of species i with Z_i protons and N_i neutrons. The equilibrium is established in a volume V_{ext} (or at a density ρ) and at a temperature T. Every particle moves freely in the volume V left over from the external volume V_{ext} after subtracting the volume occupied by each particle

$$V = V_{ext} - \sum_i n_i V_i \qquad \rho = (\overline{N} + \overline{Z})/V_{ext} \qquad (4)$$

where V_i is the i^{th} particle's volume. So the point-like particles move freely in a reduced volume V with the density determining the chemical equilibrium of $\rho_{pt} = (\bar{N} + \bar{Z})/V$. For fermions we have

$$\lambda_i^3 n_i / g_i V = (2/\pi^{1/2}) F_{FD}(\nu_i) \qquad i = p,n,{}^3He,t,{}^5Li^*,... \tag{5}$$

where

$$\lambda_i = h/(2\pi m_i kT)^{1/2} \tag{6}$$

is the thermal wavelength of the ith particle with mass m_i. The spin degeneracy factor $g_i = 2S_i + 1$. The chemical potential of the ith particle is μ_i,

$$\nu_i = \beta\mu_i = \mu_i/kT \tag{7}$$

and

$$F_{FD}(\nu_i) = \int_0^\infty dx\, x^{1/2}/(\exp(x - \nu_i)+1). \tag{8}$$

We use the function $F_{FD}(\nu)$ as tabulated in the literature [see ref. 28]. For bosons we have

$$n_i = 1/(\exp(\alpha_i)-1)+(g_i V/\lambda_i^3) F_{BE}(\alpha_i) \qquad i = d,{}^4He,d^*,.... \tag{9}$$

where $\alpha_i = -\beta\mu_i$, the first term gives the number of condensed particles, and[28])

$$F_{BE}(\alpha) = \sum_{n=1}^{\infty} \exp(-n\alpha)/n^{3/2}. \tag{10}$$

The constraint of chemical equilibrium implies that the chemical potential

$$\mu_i = Z_i\mu_p + N_i\mu_n + E_i \tag{11}$$

where

$$E_i = Z_i m_p c^2 + N_i m_n c^2 - m_i c^2 \tag{12}$$

is the binding energy of the cluster (Z_i,N_i).

Figure 5 shows the deuteron-to-proton ratio as obtained from the quantum statistical calculation[29]). The curves are labeled by the point particle densities, $\rho_{pt}/\rho_0 = 0.5$ and 0.1, corresponding to breakup densities $\rho_{bu}/\rho_0 \approx 0.32$ and 0.09, respectively; the excluded volume effects become important at high densities, $\rho_{pt} > 0.25\rho_0$, only. The value of R_{dp} in chemical equilibrium is given by the curve labeled $R_{dp}^{primordial}$. In contrast to expectations from the data, R_{dp} is not much smaller than unity, but in fact approaches one at $S/A \approx 2$. However, due to the decay of the particle unstable nuclides, R_{dp} drops substantially after the fragments have been emitted from the system. It has to be emphasized that R_{dp}^{final} is nearly independent of the exact value of the breakup density[25,29]) and that $S(R_{dp})$ varies by about 10%, although the point-particle densities vary by a factor of 5. Another important result is the maximum value of $R_{dp}^{final} \approx 0.4$ at entropies $S/A \approx 1.5$-3.5. Therefore, the entropy is not a well-defined function of R_{dp}, but it is multivalued. The rise of "S" (eq. (1)), or depletion of R_{dp}

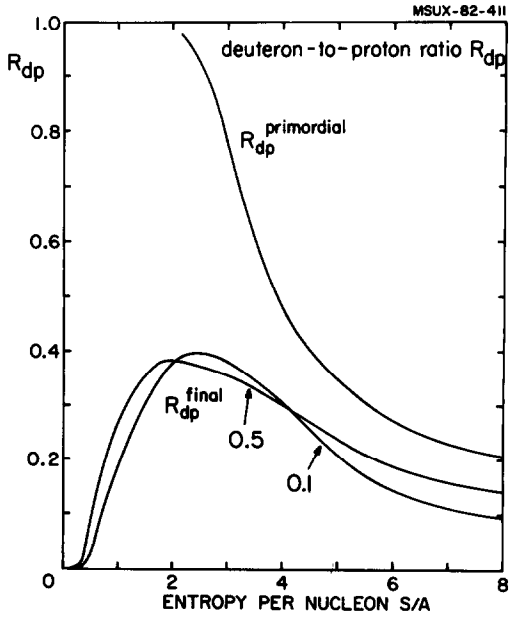

Fig. 5

predicted[25]) to occur at intermediate energies $E_{LAB} \lesssim 100$ MeV/n, has indeed been observed recently[12]) and lends support to our calculation. The triton (and ^{3}He)-to-proton ratios R_{tp} and $R_{^3Hep}$ show a very similar dependence on the entropy S/A as R_{dp}[29]). They exhibit a maximum $R^{max}_{^3Hep} = R^{max}_{tp} \approx 0.3$ around S/A $\approx$ 2-3, and are also nearly independent of the breakup density ρ_{bu}. The calculated R_{tp} values agree well with the data[29]). Hence we come to the following conclusion: although R_{dp}, R_{tp}, and $R_{^3Hep}$ are multivalued functions of S/A, they can be used to extract entropy values from the data in the high energy ($E_{LAB} > 400$ MeV/n) and low energy regimes ($E_{LAB} \lesssim$ 100 MeV/n).

The independence of the ratios on the breakup density ρ_{bu} eliminates the only unknown parameter, ρ_{bu}, from the calculation. It should be kept in mind, though, that the entropy per nucleon S/A depends on whether the matter from which the fragments are formed has actually participated in the violent interaction or whether it has been a projectile or target spectator. Therefore, we expect a distribution of entropy values in coordinate as well as in momentum space even in a single collision; the entropy can be defined only at a given location in phase space (i.e. the mean entropy of the "shocked" participant matter, the entropy of the projectile-like fragments and target-like fragments, etc.) In the regime

$100 < E_{LAB} < 400$ MeV/n corresponding to $S/A \sim 1.5 - 3$, however, R_{dp}, R_{tp} and $R_{^3Hep}$ reach plateaus and are independent of the entropy per nucleon. Here we must look for a different messenger which may provide information on the entropy.

The ^{4}He-to-proton ratio, $R_{\alpha p}$, shown in fig. 6 is a monotonically decreasing function of S/A and is also independent of the breakup density. But the plateau at $S/A \approx 0.5 - 2$ limits the applicability of $R_{\alpha p}$ for entropy measurements in the intermediate energy regime. Another proposal has been to study the ratio of "deuteron-like"-to-"proton-like" particles, $R_{"d"z}$[21], i.e. the ratio of observed correlated nucleon pairs in light clusters $(1 \times d + \frac{3}{2}(t + {}^3He) + 3 \times {}^4He)$ to the total number of observed protons (including bound protons). It has been shown[21] that $R_{"d"z}$ can be related to the entropy via eq. (1) without the assumption of a small yield of clusters, if the formation of particle unstable clusters is neglected as in ref. 23.

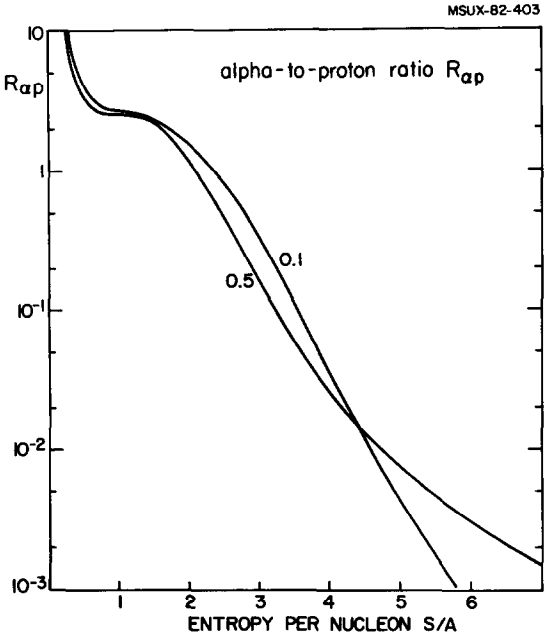

Fig. 6

The primordial $R_{"d"z}$, which only includes the ground states of the nuclides $2 \leq A \leq 4$, and the finally observable $R_{"d"z}$, which also includes the decay products, is shown as a function of the entropy in fig. 7. We observe qualitatively the same behavior as for R_{dp}: $R^{final}_{"d"z}$ is strongly affected by the decay of excited clusters and is <u>not</u> directly related to S/A via eq. (1). We can use fig. 7 to

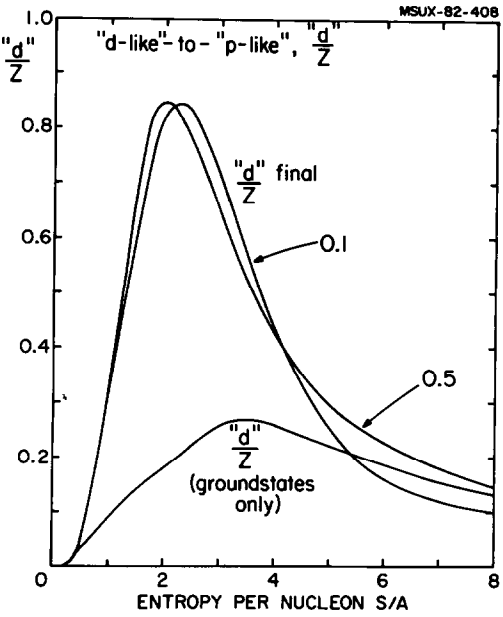

Fig. 7

determine the produced entropy graphically from the measured "d"/z ratio. It is essential to point out that the decrease of $R_{"d"z}$ below $S/A \approx 2$ is due to the condensation of the matter into fragments with mass $A \geq 6$, which have not been included in the definition of $R_{"d"z}$. This gives a decisive limit: we can find a direct measure for entropy values $S/A \lesssim 3$ when medium mass fragments are studied. Experimental data on the production of fragments with $A \geq 6$ are scarce, but the measurements at intermediate energies done so far show a substantial contribution of these medium mass fragments relative to the number of produced particles[1,3,5,7,8,10,11]. On the basis of existing data at low and high energies, a drastic change of the reaction mechanism can be expected at these intermediate energies[18]. Central collisions result in fusion at low energy, i.e. one and only one very heavy fragment is produced, while at high energies the multiplicity of charged particles (mostly protons) in central collisions can even exceed the total number of protons initially present in projectile and target (due to pion production). This also implies that single particle inclusive measurements, although sufficient for kinematically complete experiments at low energy, miss many of the details of the reaction processes at high energies[30-32].

2. Multifragmentation--evidence for a transition in the reaction mechanism at $E_{LAB} \approx 60$ MeV/n

A recent 4π event-by-event analysis of ^{12}C-induced reactions at 50-100 MeV/n on Ag and Br shows the following important features[10]): a large fraction (≈20%) of the reactions have high multiplicites ($M \geq 11$) of charged light and medium mass ($A \leq 11$) fragments.

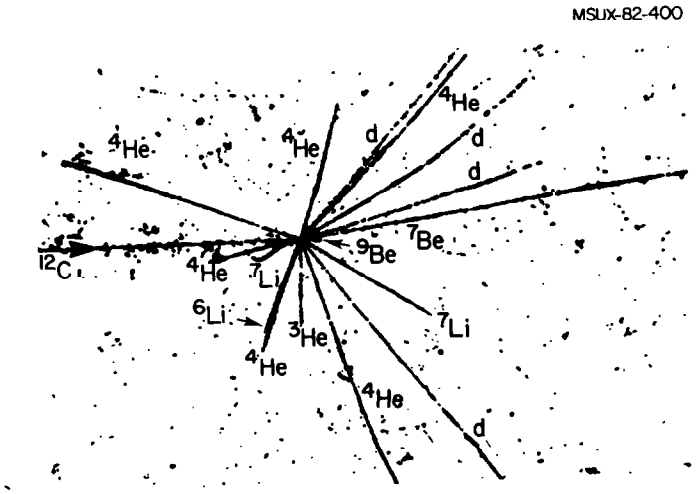

Fig. 8

Complete disintegration of the projectile and target nuclei into light and medium mass fragments is found to dominate these high multiplicity events at energies as low as 60 MeV/n. Fig. 8 shows an emulsion picture[10]) of a typical event. A ^{12}C nucleus enters from the left with an energy of 70 MeV/n. It undergoes a reaction with an Ag or Br nucleus, which results in the emission of 16 visible charged particle tracks (4 deuterons, 7 alpha particles, 3 lithium and 2 beryllium fragments) containing a total of ≈71 nucleons. In the case of a C + Br event, this corresponds to a complete breakup of the system into fragments with $A \leq 11$. If the target is Ag, a fragment with $Z \approx 18$ should be added. It is noteworthy that this is not a rare type of event. In this sample of 73 events with $M \geq 11$ studied in ref. 10, corresponding to 20% of the total reaction cross section, several events with even higher charged particle multiplicity and/or number of emitted charges have been observed. These findings yield direct evidence for the transition from fusion to "multifragmentation" in the intermediate energy regime. It also casts strong doubts on the selection or identification of central events by fission fragment correlation measurements[11,13]) at these rather high energies. The data[10]) indicate that no residual nucleus is left to fission once the light and medium mass fragments are subtracted from the sum of projectile

and target masses. This phenomenon has also been observed at somewhat higher energies[34]). These multifragmentation events do not show any "leading particles", i.e. fragments in the forward direction with a speed close to the beam velocity are not observed. Of the 16 visible ejectiles in fig. 8, only one fragment has an energy exceeding 15 MeV/n; however, this deuteron of 50 MeV/n is emitted at $\theta_{LAB} = 49°$ and so is not due to projectile fragmentation either. The remaining 15 fragments have energies 1 MeV/n-14 MeV/n. Therefore, the projectile must have stopped completely in the target. The blob of excited nuclear matter thus formed disintegrates totally into light and medium mass fragments in contrast to the two massive fragments observed in ordinary fission fragment distributions. The opaque multifragmentation events[10]) bear a surprising resemblance (e.g. in their emission pattern) to those predicted by the fluid dynamical model at intermediate energies[15,16,35]). Once central events are selected, the projectile is essentially stopped in the target and the subsequent explosion of the combined systems results in a predominant sidewards emission of the fragments due to collective flow effects. Even for intermediate impact parameter collisions, a substantial transverse momentum transfer to the remnants of the projectile is predicted--the bounce-off effect[31,32,35-37]). This means that particles with large velocities should be observable at rather large angles.

The lack of transparency observed in central collisions[10]) is in marked contrast to the ∿30% drop of the total reaction cross section reported in the same energy regime[38,5]). We conclude that the latter is due to surface transparency effects in peripheral collisions. Central collisions apparently probe the bulk stopping power of dense nuclear matter, which increases when going from low to intermediate energy. We want to emphasize the decrease of the average size of the emitted fragments over the region from medium to high energies. This reflects the competition between maximizing the entropy and minimizing the internal energy: the statistical equilibrium state of minimum Helmholtz free energy

$$F = E - TS \tag{13}$$

is established by forming more massive fragments at temperatures comparable to or lower than the binding energy. Here the gain in binding energy exceeds the decrease of the entropy. The number of degrees of freedom is increased by breaking up most of these

correlations at high temperatures; thus it is advantageous to produce light fragments, in particular free protons and neutrons at high bombarding energies.

3. Evidence for a liquid-vapor phase transition

The temperature drops substantially during the isentropic expansion (see fig. 2) from the initial dense state. Hence, in the late stages of the reaction, where the composite fragments are formed, the temperature varies strongly with the breakup density. The pressure $P(\rho,T)$ of the nuclear medium is shown in fig. 9 for low densities $\rho/\rho_0 < 1$ and for typical breakup temperatures $T<40$ MeV[29]). We observe that $P(\rho,T)$, the pressure at constant temperature, exhibits local maxima and minima, i.e. a van der Waals behavior, typical of a medium with long range attractive and short range repulsive forces between the constituents. The nuclear equation of state exhibits a critical point at $\rho \approx 0.4\rho_0$ and $T_c \approx 18$ MeV; thus the nuclear equation of state shows the characteristics of a liquid vapor phase transition at low densities[39-42,29]). The nuclear equation of state shown in fig. 9 can be approximated in the vicinity of the critical point by the van der Waals equation of state

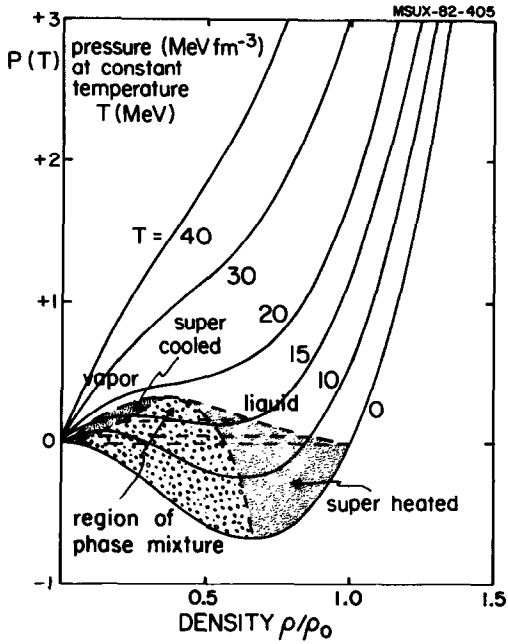

Fig. 9

$$P = -\left(\frac{\partial F}{\partial V}\right)_{T,N} = \frac{T}{\frac{V}{N} - b} - \left(\frac{N}{V}\right)^2 a \tag{14}$$

with the modified Helmholtz free energy

$$F = -NT(\ell n(n_Q(V - Nb)/N) + 1) - \frac{N^2 a}{V} \tag{15}$$

Here b represents the hard core excluded volume of the nucleon and $(N/V)^2 a$ is the internal pressure due to the long range nucleon-nucleon interaction. The law of corresponding states

$$\tilde{P} = \frac{\frac{8}{3}\tilde{T}}{\tilde{V} - \frac{1}{3}} - \frac{3}{\tilde{V}^2} \tag{16}$$

is obtained by substituting

$$\begin{aligned} P_c &= a/27\ b^2 \\ V_c &= 3Nb \\ T_c &= 8a/27b\ , \end{aligned} \tag{17}$$

the critical pressure, volume and temperature at the critical point, respectively, and rewriting eq. (14) in terms of the dimensionless variables $\tilde{P} = P/P_c$, $\tilde{V} = V/V_c$ and $T = T/T_c$. At the critical point, $\tilde{P} = \tilde{V} = \tilde{T} = 1$, the isothermal $P(\tilde{V},T)$ has a saddle point, while for $\tilde{T} > 1$ the isothermal pressure $\tilde{P}(\tilde{V},\tilde{T} = \text{const})$ is monotonic. The liquid-vapor phase separation no longer exists and this phase is therefore called the fluid phase.

A liquid phase and a vapor phase can coexist in a well determined density regime once the temperature is less that the critical temperature, $T < T_c \approx 18$ MeV, i.e. $\tilde{T} < 1$ (the shaded area in fig. 9). The condition for thermodynamic stability of the two phase system is

$$T_{liquid} = T_{vapor} \tag{18a}$$

$$P_{liquid} = P_{vapor} \tag{18b}$$

$$\mu_{liquid} = \mu_{vapor} \tag{18c}$$

corresponding to thermal, mechanical and diffusive equilibrium between the two phases. Eq. (18c) is equivalent to requiring the Gibbs free energy

$$G(T,V,N) = NTV/(V - Nb) - 2N^2 a/V - NT\ \ell n(n_Q(V - N\,b)/N) \tag{18d}$$

to be the same in the liquid and vapor phases. Hence the Maxwell

construction of the isothermal coexistence curve P(V,T=const) (dashed horizontal lines in fig. 9) implies that the chemical potential of the strongly interacting nucleons in the liquid phase is equated to the chemical potential of the nucleons in the free gaseous phase. In order for such a liquid vapor phase transition actually to occur in the final state of a central nuclear collision, the relaxation time for the phase equilibration must be shorter than the time during which the system expands and thermal contact between the constituents ceases. However, the time necessary for a fragment to separate from the remainder of the exploding system is of the same magnitude as the explosion time itself (0.5×10^{-21}sec)[32]. This means also that we expect a competition of particle emission from the surface of the system during the expansion with the volume breakup of the remaining system, which has reached too low a density to ensure thermal contact[32]. Since we cannot answer the question of the occurrence of a liquid vapor transition conclusively, we will discuss here an observable consequence, which can allow an experimental detection of such a two phase equilibrium[29].

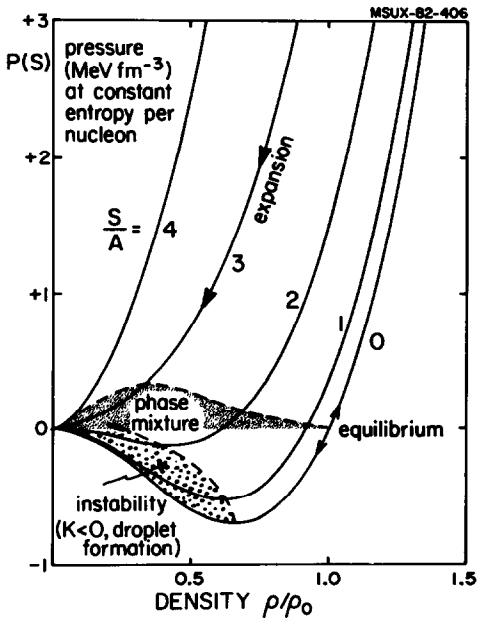

Fig. 10

As we have discussed above, the entropy of the system remains unchanged during the expansion stage. Fig. 10 shows the pressure $P(\rho,S)$ as a function of the density, but now at constant entropy S

compared to fig. 9, where the temperature was kept constant. We observe that for entropies as high as $S/A \lesssim 3$, the isentropic expansion always merges the regime labeled "phase mixture", i.e. we may expect effects of a possible liquid vapor phase transition up to bombarding energies of several hundred MeV/n. However, if the system actually undergoes the phase transition, the entropy will not stay constant. The volume increases at constant T when going from the liquid to the vapor phase and the latent heat of vaporization is released. For a system consisting of nucleons only the entropy increase is seen immediately from the Sackur-Tetrode equation,

$$\frac{S}{A} = \frac{5}{2} + \ell n \left(\frac{n_Q}{\rho}\right) \tag{19}$$

with the quantum concentration of the nucleons

$$n_Q = \left(\frac{m_N T}{2\pi\hbar^2}\right) . \tag{20}$$

When the volume increases (the density decreases) at constant temperature, the entropy increases as

$$\frac{\Delta S}{A} = \ell n\ \rho_{vapor} - \ell n\ \rho_{liquid} \tag{21}$$

The latent heat of vaporization thus released is

$$L = T(S_{vapor} - S_{liquid}) \tag{22}$$

i.e. the latent heat (and the entropy increase) are given by the density difference between the two sides of the phase coexistence region. This entropy increase associated with a liquid vapor phase transition should be observable via a characteristic change of the entropy excitation function[29]. At high enough bombarding energies $E_{LAB} \gtrsim 1$ GeV/n, the entropy produced exceeds $S/A \approx 3$, hence the liquid vapor phase transition region cannot be reached. The system stays above the critical point. Although the initially produced entropy drops smoothly when the bombarding energy is lowered (see fig. 4), we expect a rise of the finally observed entropy as soon as the critical point is reached. Then the additional entropy production will be larger, the smaller the initial entropy has been, because the volume change associated with the liquid-vapor phase transformation gets bigger and bigger. In fact, if a liquid vapor coexistence occurs, the entropy is predicted[29] to exhibit a minimum at about $S/A \approx 3$ ($E_{LAB} \sim 400$ MeV/n) and then even rises to $S/A \approx 4$ as the energy is lowered to $E_{LAB} \lesssim 200$ MeV/n. This can be observed by measuring medium mass fragments, e.g. the alpha-to-proton ratio,

$R_{\alpha p}$, in central collisions (i.e. in high multiplicity selected events).

The entropy values extracted via fig. 6 from the recent inclusive measurements of $R_{\alpha p}$[12]) do in fact imply entropies $S/A \gtrsim 3$ in the whole intermediate bombarding energy regime[29]) which seems to be indicative of a liquid vapor phase transition (see fig. 4). However, first 4π data obtained with the plastic ball demonstrate that the fragment yield ratios in central events can differ substantially from the inclusive data[43])--hence we have to wait for the appropriate 4π $R_{\alpha p}$ excitation function before we can come to a definite conclusion.

4. Evidence for condensation phenomena--the charge distribution of fragments

Another method to obtain information about a liquid-vapor transition is the yield of fragments heavier than alphas, e.g. Be, C, O and even heavier fragments. To study the mass distribution of these medium heavy fragments, let us first step back from the detailed quantum statistical model[29]) described above and neglect complicating effects such as Fermi energies, Bose condensation, excluded volumes, metastable particles, Z and N dependence of binding energies, spins and thus degeneracies, etc. Then an analytical expression for the fragment charge and mass distribution can be derived using the droplet model of condensation[44]). We assume that the binding energy of a nucleus is given by a volume and a surface term only,

$$E_B = a_V A - a_S A^{2/3} \tag{23}$$

with the volume coefficients $a_V \approx 16$ MeV and the surface tension coefficient $a_S \approx 13$ MeV. Then the distribution over droplet sizes A is given by[44])

$$Y(A) = a_0 n_Q V A^{-7/3} \exp[(E_B(A)+A\cdot\mu)/T] \tag{24}$$

where a_0 is a normalization constant and n_Q is the quantum concentration of the nucleons defined above, eq. (20). After inserting eq. (23) into eq. (24), we obtain

$$Y(A) = a_0 n_Q V A^{-7/3} x^{A^{2/3}} y^A \tag{25}$$

where

$$x = \exp(-a_S/T) \tag{26}$$

is a measure of the temperature, and

$$y = \exp[(a_V + \mu)/T] \tag{27}$$

is directly related to the density via the chemical potential μ. The picture of fragment formation at low temperatures ($x < 1$) is that of vapor approaching the point of condensation. At low enough densities $y \ll 1$, the system will consist of separated nucleons predominantly, with fragments of two, three or more nucleons bound together forming and decaying in statistical equilibrium with the other fragments. Rather large nuclei resembling droplets of the liquid phase can form, but in general they will occur less frequently than light fragments. If the density is raised at constant, low temperature--it becomes energetically advantageous for the nucleons to form composite fragments and for the fragments to grow further by amalgamation, thus lowering the surface energy. At low enough temperatures and high enough density it is most favorable for the nuclei to grow to "macroscopic" large fragments. Massive fragments represent the liquid phase--hence their presence indicates the onset of condensation.

Let us recapitulate the situation quantitatively, making use of eq. (25). At temperatures below $T_c \approx a_s \approx 14$ MeV, x is small; and at low densities y is also small. Hence Y(A) decreases exponentially with increasing fragment mass A. At the critical point, y=1 and x=1, and Y(A) decays as $A^{-7/3}$ (see ref. 45). At higher density, $y > 1$, but at temperatures below the critical point, $x < 1$, we enter the condensation region. The mass yield decreases at first, i.e. for small mass fragments, but it increases again for heavier fragments as soon as the increase in y^A dominates the function Y(A). This increasing probability for producing very large fragments indicates, as discussed above, that condensation has indeed taken place. In fact, for infinite systems, Y(A) would diverge as y^A for $A \to \infty$. In conclusion, if condensation occurs we expect a rapid falloff of the light fragment yield, with a minimum at a critical A_{crit}, above which Y(A) rapidly increases.

Figure 11 shows the charge distribution Y(Z) for $Z < 14$ as observed in high multiplicity selected events[10]). A nearly exponential falloff of Y(Z) can be seen. Also shown are the results of the quantum statistical model discussed above[29]). The exponential decrease of Y(Z) is observed for both entropies considered, S/A = 2.6 and 1.5 (the calculation has been performed at $\rho_{pt}/\rho_0 = 0.3$). However, the slope of Y(Z) is directly related to the entropy: as the entropy is increased, the charge distribution falls off much more rapidly. Since the yield of, e.g., nitrogen fragments increases by two orders of magnitude when S/A is decreased from 2.6

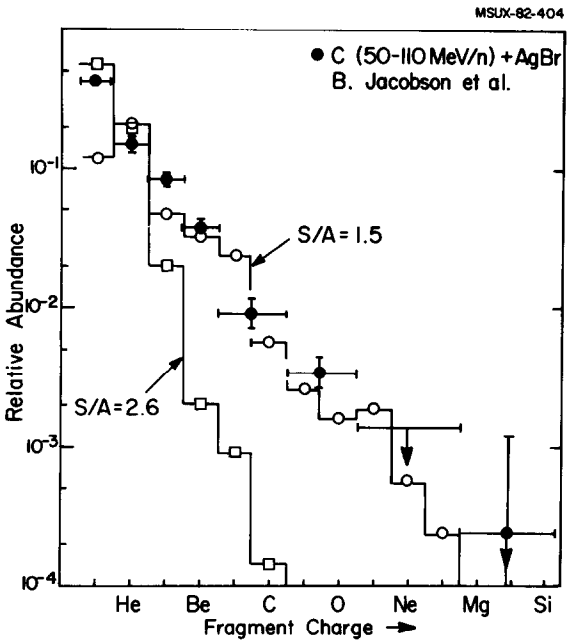

Fig. 11

to 1.5, Y(Z) promises to be a real entropy meter once medium mass fragments are measured. More important, however, than the expected nearly exponential falloff is the fact[10]) that the charge distribution exhibits a minimum around Z = 10 and then rises to a broad maximum at Z = 15-35 (not shown in fig. 11); hence, Y(Z) (and, because A ≈ 2Z, also Y(A)) exhibits a Z-dependence characteristic of the onset of condensation. This is a very encouraging result which gets further support from the fact that the A values at the maximum of Y(A) do not resemble typical target fragmentation or fission values. Since the A distribution at large A has been determined by missing mass considerations, an experiment specifically designed to measure Y(A) directly at all A will be of great importance to study this question more quantitatively in the future.

5. Fragmentation in the superheated liquid phase

Consider now a second possibility for the breakup of the expanding system: the expansion is so rapid that the two phase equilibrium cannot be established. Then the expansion proceeds along curves of constant entropy into the domain of meta stable superheated states shown in fig. 9. This regime is exceptional also

in the sense that it exhibits negative pressures. No law of nature, however, forbids the existence of such a state. It will however be a transient state, since by construction the two phase equilibrium is the state of largest entropy and lowest free energy and thus the thermodynamically absolutely stable state. The system will expand until it reaches the minimum in $P(\rho,T)$ or $P(\rho,S)$ where it becomes mechanically unstable. This is the case if the isothermal compressibility coefficient

$$K = \rho(\partial P/\partial\rho)_{T=const} \tag{28a}$$

or the isentropic compressibility coefficient

$$K = \rho(\partial P/\partial\rho)_{S=const.} \tag{28b}$$

become negative[32,40,46]--hence it will break up into pieces of a size determined by the mass distribution in the superheated state. Therefore the observed fragment mass distribution will again be given by eq. (25). The critical radius R_c for nucleation of a droplet in the superheated liquid can be calculated from the difference of the Gibbs free energy of the liquid and the vapor phase. (Since the liquid is superheated, $G_{liquid} \neq G_{vapor}$, in contrast to the situation in phase equilibrium). Furthermore the surface free energy of a small liquid droplet is positive, and therefore its free energy is larger than the free energy of the bulk fluid, which in turn is smaller than the free energy of the surrounding vapor. At small droplet radii R the droplet may thus be unstable with respect to vaporization. The Gibbs free energy difference for droplets is given by

$$\Delta G = G_{liquid} - G_{vapor} = -\frac{4}{3}\pi R^3 \cdot \rho \cdot \Delta\mu + 4\pi R^2 a_S \tag{29}$$

where $\Delta\mu$ is the chemical potential difference between a nucleon in the liquid and a nucleon in the vapor. ΔG reaches a maximum at $d\Delta G/dr = 0$, i.e. at

$$R_c = \frac{2a_S}{\rho \cdot \Delta\mu} \tag{30}$$

Nuclei with $R < R_c$ tend to evaporate, nuclei with $R > R_c$ tend to grow spontaneously. The free energy barrier which has to be overcome for a nucleus in order to grow beyond R_c is given by

$$G_{crit} = \frac{16\pi}{3}\left[a_S^3/(\rho\Delta\mu)^2\right] \tag{31}$$

Hence we expect the minimum discussed above in the fragment mass distribution to be determined by the critical droplet size given by eq. (30).

6. Indications for collective flow effects

Up to now we have only discussed nuclear fragment emission. However, even at energies as low as $E_{LAB} < 80$ MeV/n (far below the n-n threshold) pion production has been observed experimentally[47]. Since pion production can be used as a sensitive tool to probe nuclear matter[15,25,32,40], we want to discuss briefly the high multiplicity selected experimental data obtained at higher energies[33].

The number of pions per emitted charged nuclear fragment, $\langle n_{\pi^-} \rangle / \langle Q \rangle$, is shown in fig. 12 as measured in high multiplicity selected collisions of Ar + KCl[33] as a function of the bombarding energy. We observe that a simple fireball calculation (dashed) overestimates the pion production by factors of 3 and more, since apparently too much energy is stored into the thermal degrees of freedom. Also cascade calculations[20] overestimate the number of pions considerably, in particular at $E_{LAB} \leq 800$ MeV/n. (The difference between the cascade calculation and the data may be useful for extracting the compression energy at high density[15,40,48].) On the other hand, the non-viscous fluid dynamical calculation underestimates the number of produced pions: too much of the internal excitation energy is transferred into collective fluid flow[23,25]. The inclusion of viscous effects into the hydrodynamic calculation increases the thermal energy and the calculated pion yield (fig. 12, full curve)[25] is in good agreement with the experimental data[33]. These results provide some indication for the occurrence of collective flow in nuclear collisions. Some additional evidence can be

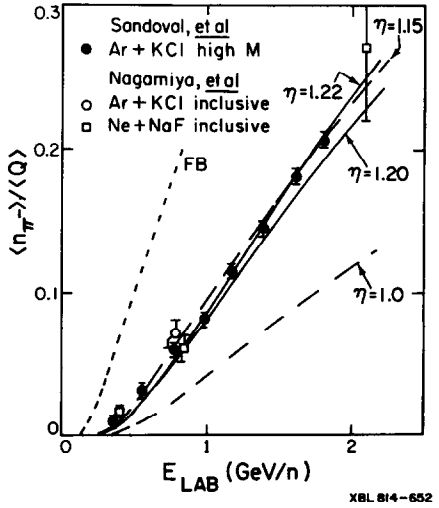

Fig. 12

obtained from the angular distributions of fragments emitted in high multiplicity triggered inclusive experiments.

The double differential cross sections of light fragments emitted from nearly central--i.e. high multiplicity selected--collisions have been measured recently[49] and compared to the different models discussed above[31,36] (see fig. 13). The angular distributions of protons emitted in central collisions of Ne (393 MeV/n) on U

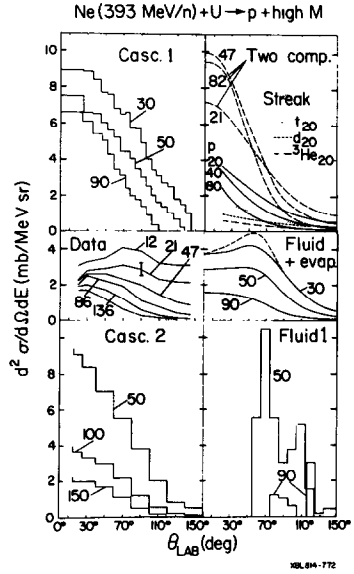

Fig. 13

exhibit broad sidewards maxima (middle left frame of fig. 13). The numbers in the figure indicate the proton kinetic energies. Cascade calculations[36] yield forward-peaked angular distributions, even if central collisons are selected (upper and lower left frame). Hydrodynamic calculations without thermal breakup yield too narrow sidewards peaks (lower right frame)[36]. The simplified two component and firestreak models (upper right frame) give similar results as the complex three-dimensional cascade calculations, but since they are also forward peaked, they also disagree with the data. On the other hand, the fluid dynamical model with final break-up included[36] (middle right frame) gives a reasonable description of the observed forward suppression and also reproduces qualitatively the forward shift of the position of the sidewards maxima with proton energy.

Early experiments using Ag Cl detectors[50] showed sidewards peaking in the angular distribution of emitted α-particles, which

should exhibit the signs of the collective flow more distinctively than protons because of the smaller thermal velocities. For a conclusive answer to the question of signatures of collective flow in double differential cross sections, detailed investigations on the emission of nuclei heavier than protons are necessary. An independent indication for collective flow effects has recently been found in a two-particle correlation measurement[37b]. A fast sidewards moving proton evidently is preferentially emitted in coincidence with another proton moving in the same direction ("jetting phenomenon"[31,36,37]) rather than in the opposite direction (as simple knockout models would suggest).

7. Flow pattern recognition in 4π exclusive experiments

A more recent idea on how the collective flow can be observed is sketched briefly in this last chapter, viz. the "global" momentum tensor analysis. This analysis can be done experimentally only in 4π detector systems such as emulsion, streamer chamber, or the plastic ball. The basic idea is to measure simultaneously on an event-by-event basis all (charged) particles and determine all the associated momenta. This is indeed a formidable task! Once this information is available, one can transform all the physical quantities into the center-of-momentum frame and determine the direction of maximum momentum and energy flow by performing a principal axis transformation in analogy to the moment of inertia tensor. The various concepts which have been proposed to analyze nuclear collisions are thrust[36,51,52], sphericity[52-54], and kinetic energy flow[53,54]. The longitudinal energy degradation is another variable proposed[55]. The first two concepts have been adapted from high energy physics, but they have the disadvantage of being non-analytic[51] or do not take into account the emission of composite particles properly[52]. The energy flow tensor[53,54],

$$F_{ij} = \frac{1}{N} \sum_{\nu} \frac{p_i(\nu) p_j(\nu)}{2m_\nu} \tag{32}$$

is a generalization of the sphericity concept, which allows for an appropriate weighting of composite fragments relative to nucleons.

By comparing the results of the cascade and the hydrodynamic calculation, we want to determine the sensitivity of the global variables discussed above to the collision dynamics. We observe a much larger transverse momentum transfer--the bounce-off effect--in the hydrodynamic calculation than in the cascade. This

is the consequence of a strong pressure buildup in the fluid which pushes the residual fragments apart. The single n-n collisions present in the cascade model result in a much smaller momentum transfer. Hence we expect that the largest principal axis of the flow tensor is rotated to a larger angle for the fluid dynamical calculations than for the cascade.

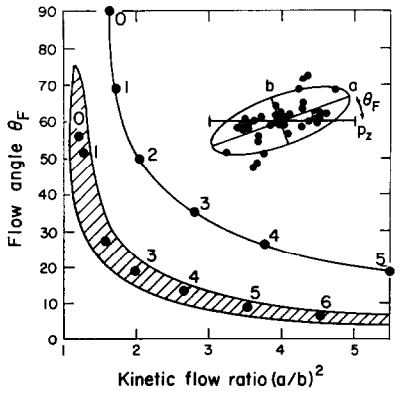

Fig. 14

In order to amplify this difference we propose[53,54]) to plot the flow angle θ^{CM}_{flow} versus the aspect ratio R_{13}, i.e. the ratio of the largest to the smallest principal axis of the flow tensor. $R_{13}>>1$ reflects events stretched in momentum space, while $R_{13}=1$ indicates a spherical momentum distribution. The ridge in the θ_{flow}-R_{13} plane depends on the total mass of the system--cascade calculations show that substantial flow angles should only be expected for very heavy systems $A_1=A_2>100$. The results of these cascade calculations for the system U+U at $E_{LAB}=250$ MeV/n are shown in fig. 14[53]). Also shown are the results of the fluid dynamical calculation[54]). A qualitatively similar ridge with, however, larger deflection angles and aspect ratios R_{13} can be seen; the matter flux is apparently more strongly correlated in the hydrodynamical model. A detailed study of the impact parameter dependence of the flow angle $\theta=\arccos([e_3]_Z/e_3)$, aspect ratio $R_{13}=Q_1/Q_3$, sphericity $S=\frac{3}{2}(Q_1+Q_2)$ and coplanarity (flatness) $C=\sqrt{3/2}\ (Q_2-Q_1)$ with the principal values $Q_1<Q_2<Q_3$ (normalized by $(\mathrm{Tr}\ F_{ij})^{-1}$) of the flow tensor as resulting from the hydrodynamic model calculation is given in ref. 54.

The general behavior of the flow pattern in the fluid dynamical model is as follows: the flow angle rises smoothly from 0° at large impact parameters to 90° at b=0, while sphericity and coplanarity rise from 0 to 0.9 and 0.2 respectively. Since the matter flow

reflects the longitudinal, $p_{||}$, and transverse, $p_{\perp}$, momentum transfer in a collision, it can be used to directly measure the pressure built up in the high density stage of the reaction[56])

$$p_{\perp} = \int_t \int_f P(\rho,S)\, d\vec{f}\, dt \qquad (33)$$

where the total pressure is the sum of an interaction pressure $P_C(\rho,S=0)$ and a kinetic Fermi gas term $P_T(\rho,S>0)$.

$$P(\rho,S) = P_C(\rho,S=0) + P_T(\rho,S>0) \qquad (34)$$

The bombarding energy dependence of $(P_C + P_T)/P_T$, i.e. the ratio of the total pressure to the Fermi-gas term in eq. (34) is shown in fig. 15. Two results must be pointed out[17]): First, we observe a

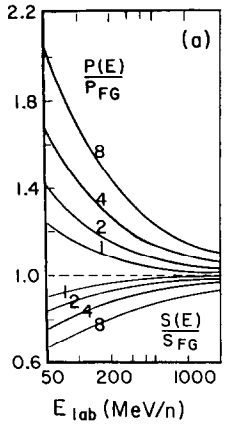

Fig. 15

strong bombarding energy dependence of $P/P_T(E_{LAB})$. The kinetic term P_T dominates at high energies $(P \to P_T)$, while the interaction term P_C far exceeds P_T at intermediate energies, $P>>P_T$. Second, we find a remarkable sensitivity of the total pressure to the stiffness of the nuclear equation of state at high density: the pressure depends directly on the nuclear compressibility as indicated by the different curves in fig. 15. The discrepancy in P resulting from the different compressibilities is particularly notable at energies $E_{LAB} \lesssim 200$ MeV/n. Since the flow characteristics depend directly on the pressure, we can expect a dependence of the flow pattern on the stiffness of the equation of state. We have investigated the bombarding energy dependence of the kinetic flow ratio R_{13}

for central collisions of U + U, using the fluid dynamical model.

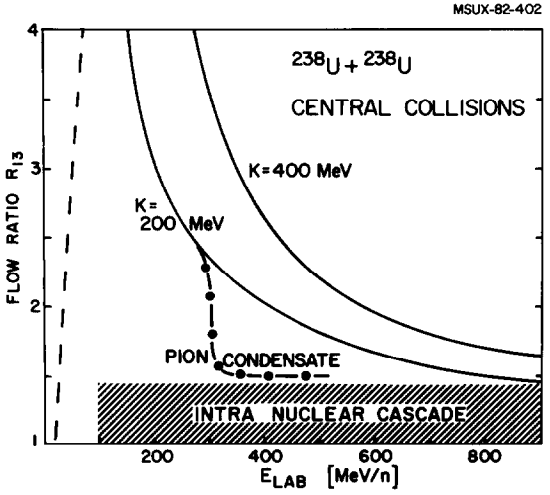

Fig. 16

Figure 16 shows the most important results of our calculation. We find a strong energy dependence of $R_{13}(E_{LAB})$, which indeed closely reflects the energy dependence of $P/P_T(E_{LAB})$ discussed above. This is in stark contrast to our cascade calculations[53,54], which show no indications for a dependence of R_{13} on the bombarding energy, even for the heavy system U + U (shaded area in fig. 16). In fact, this is what we should expect from the cascade calculation--even for very heavy systems it can at the most resemble the kinetic pressure P_T of the nucleons,[32] effects of the nn interactions, i.e. the pressure $P_C(\rho)$, are not incorporated into this model. Hence, the values $R_{13}^{cascade} \lesssim 1.4$ are close to the thermalized "fireball" momentum distribution. The strong collective flow observed in the hydrodynamical calculations is not seen. At high energies, $E_{LAB} \gtrsim 1$ GeV, the two approaches do not yield drastically different results for R_{13}. The flow angles, θ^{flow}, deviate however, even at high energies. The cascade predicts smaller emission angles than fluid dynamics. Quasi-free nucleon-nucleon collisions, which occur in the nuclear surface even for central collisions, are neglected in the fluid dynamical model due to its zero mean free path assumption.

Some unexpected findings of the first event-by-event analysis of 4π exclusive experiments[57-60] should be pointed out in this respect. The observed transverse momentum transfer and flow angles considerably exceed the corresponding cascade simulations, even for systems as light as Ne + NaF and Ar + KCl at energies between

0.4 and 1.8 GeV/n[58-60]. The largest deviations from the cascade predictions seem to emerge for the heaviest system studied to date, Ar + Pb at 0.4 and 0.8 GeV/n[58,59], in particular with average flow angles exceeding the maximum predicted flow angle in the cascade by more than 50%[59]! Whether this presents further evidence for hydrodynamic flow remains to be studied in more detailed investigations.

Theoretically, the change of $R_{13}(E_{LAB})$ with the nuclear compressibility is of particular importance. Fig. 16 shows $R_{13}(E_{LAB})$ for three different equations of state. As with the dependence of P/P_T on the compressibility (fig. 15)[17], R_{13} increases (at a given bombarding energy) if the compressibility (and hence $P_c(\rho)$) is increased. This can offer the unique opportunity to directly obtain experimental information on the stiffness of the equation of state at $\rho >> \rho_0$. The measurement of $R_{13}(E_{LAB})$ can even allow an experimental search for abnormal super dense states (pion condensates, density isomers[54]), which would reveal themselves by a threshold decrease of R_{13} at the critical bombarding energy E_{LAB}^{crit} sufficient for a transition into an abnormal state to occur as indicated in fig. 16. The decrease of the interaction pressure P_c may even lead to metastable, "density isomeric" states. Just above the barrier to such an abnormal state, P_c would even be negative and inhibit an immediate decay of this state. This is shown in figs. 17 and 18, which show the trapping of the matter (under the hypothesis of a density isomeric state at $\rho > 2\rho_0$) in a plot of the equation of state $E(\rho,S)$ (fig. 17)[15] and the time evolution of a

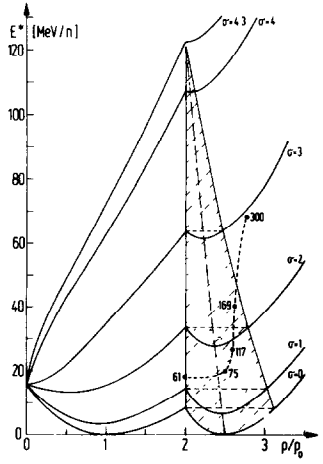

Fig. 17

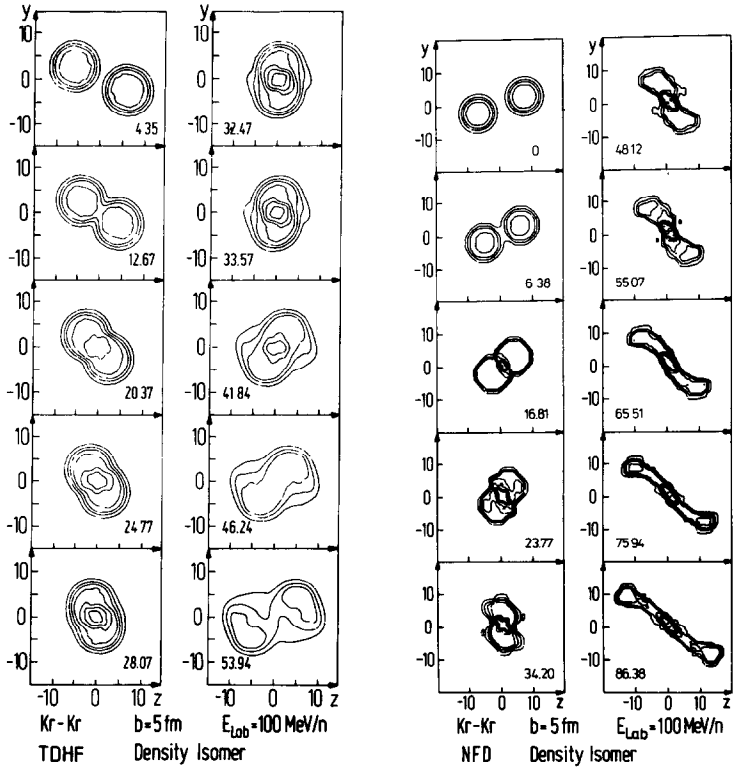

Fig. 18

noncentral collision (b = 5 fm) of two medium mass nuclei at E_{LAB} = 100 MeV/n (fig. 18). The latter figure shows a comparison[16]) of TDHF and hydrodynamic calculations, both assuming a secondary minimum in $E_c(\rho)$ as shown in fig. 17. In the TDHF calculation, the abnormal matter is formed as a short-lived transient state with lifetime τ less than the collision time. The fluid dynamical calculation, on the other hand, predicts lifetimes longer than the collision time. The consideration of such abnormal states may seem very speculative, but it will be important to explore the high density regime experimentally, since firm calculations of the behavior of nuclear matter at high densities are nearly impossible from current knowledge of ground state nuclei[66]).

8. Conclusions

We have seen that violent nuclear collisions at intermediate energies offer the possibility of studying a wealth of new phenomena related to the bulk properties of nuclei and nuclear matter. One

important question to be studied in the near future is the apparent paradox of an increased overall transparency, reflected by the strong decrease of the total reaction cross section, compared to the large nuclear stopping power and, correspondingly, short mean free path of nucleons in nuclear matter observed for central collisions, (high multiplicity selected events resembling $\sim$20% of the total reaction cross section). Collisions of heavier nuclei will be useful to study in detail the fragmentation mechanism leading to the expected high multiplicities, $M > 50-100$, which can yield information about condensation effects and a possible liquid-vapor phase transition at densities lower than ρ_0. To clarify this question it will be essential to study the formation of medium mass fragments of $A = 6-60$ in the multifragmentation events. This requires the availability of 4π exclusive detector systems, which are capable of good angular resolution and high multitrack efficiency, even for fragments with $E \lesssim 1$ MeV/n. Ultimately, such a device will be necessary to explore the flow effects in collisions, e.g. Pb(200 MeV/n) + Pb, which offers the unique opportunity to study nuclear matter properties at densities $\rho > \rho_0$. In particular, we have shown that such "jetting" experiments can be used to directly probe the compressibility of dense matter and to search specifically for phase transitions at high densities and temperatures. These are indeed challenging questions to be answered by the next generation of experiments.

References

*On leave of absence from the Department of Nuclear Physics, University of Madras, Madras 600 025, India.

1) J. Gosset, H.H. Gutbrod, W.G. Meyer, A.M. Poskanzer, A. Sandoval, R. Stock, G.D. Westfall, Phys. Rev. C16 (1977) 629
2) K. van Bibber, D.L. Hendrie, D.K. Scott, H.H. Weiman, L.S. Schroeder, J.V. Gaega, S.A. Cessin, R. Treuhaft, J.Y. Grossford, and C.Y. Wong, Phys. Rev. Lett. 43 (1979) 840
3) K.A. Fraenkel, J.D. Stevenson, Phys. Rev. C23 (1981) 1511
4) B. Jakobsson, L. Carlen, P. Kristiansson, J. Krumlinde, A. Oskarsson, I. Otterlund, B. Schroder, H.-Å. Gustafsson, T. Johansson, H. Ryde, J.P. Bondorf, G. Fai, A.O.T. Karvinen, O.B. Nielsen, M. Buenerd, J. Cole, D. Leburn, J.M. Loiseaux, P. Martin, R. Ost, F. de Saintignon, C. Guet, E. Monnand, J. Mougey, H. Nifenecker, P. Perrin, J. Pinston, C. Ristori, and F. Schussler, Phys. Lett. 102B (1981) 121

5) J. Mougey, R. Ost, M. Buenerd, A.J. Cole, C. Guet, D. Lebrun, J.M. Loiseaux, P. Martin, M. Maurel, E. Monnand, H. Nifenecker, P. Perrin, J. Pinston, C. Ristori, P. de Saintignon, F. Schussler, L. Carlen, B. Jakobsson, A. Oskarsson, I. Otterlund, B. Schroder, H.-Å. Gustafsson, T. Johnsson, H. Ryde, J.P. Bondorf, O.B. Nielsen, G. Tibell, Phys. Lett. 105B (1981) 25; and J. Mougey, Nucl. Phys. A387 (1982) 109c

6) T.C. Awes, G. Poggi, S. Saini, C.K. Gelbke, L. Legrain, G.D. Westfall, Phys. Lett. 103B (1981) 417; D.K. Scott, Nucl. Phys. A354 (1981) 375c; C.K. Gelbke, Nucl. Phys. A387 (1982) 79c

7) K.L. Wolf, Proc. V High Energy Summer Study, Lawrence Berkeley Laboratory report LBL 12652 (1981) p. 1

8) W. Loveland, P.L. McGaughey, K.J. Moody, R.H. Kraus, K. Aleklett, R.M. McFarland, and G.T. Seaborg, ibid., p. 203

9) J.B. Natowitz, M.N. Namboodiri, L. Adler, R.P. Schmitt, R.L. Watson, S. Simon, M. Berlanger, and R. Choudhury, Phys. Rev. Lett. 47 (1981) 1114

10) B. Jakobsson, G. Jönson, B. Lindquist, and A. Oskarsson, Z. Physik A307 (1982) 293; see also Lund University report LUIP 8207 (1982)

11) U. Lynen, H. Ho, W. Kühn, D. Pelte, U. Winkler, W.F.J. Müller, Y.T. Chu, P. Doll, A. Gobbi, K. Hildenbrand, A. Olmi, H. Sann, H. Stelzer, R. Bock, H. Löhner, R. Glasow, R. Santo, Nucl. Phys. A387 (1982) 129c; W.F.J. Müller, thesis, Heidelberg (1981); R. Glasow, et al., Phys. Lett., 120B (1983) 71, 108B (1982) 15

12) G.D. Westfall, B.V. Jacak, N. Anantaraman, M.V. Curtin, G.M. Crawley, C.K. Gelbke, B. Hasselquist, W.G. Lynch, D.K. Scott, M.B. Tsang, M.J. Murphy, T.J.M. Symons, R. Legrain, T.J. Majors, Phys. Lett. 116B (1982) 118

13) M. Rivet, B. Borderie, S. Song, D. Guerreau, H. Oeschler, R. Bimbot, I. Forest, J. Galin, D. Gardes, B. Gatty, M. Lefort, B. Tamain, and X. Tarrago, Nucl. Phys. A387 (1982) 143c

14) R.L. Auble, J.B. Ball, F.E. Bertrand, C.B. Fulmer, D.C. Hensley, I.Y. Lee, R.L. Robinson, P.H. Stelson, D.L. Hendrie, H.D. Holmgren, J.D. Silk, and H. Breuer, Phys. Rev. Lett. 49 (1982) 441

15) H. Stöcker, J. Maruhn, W. Greiner, Phys. Lett. 81B (1979) 303 and Z. Physik A290 (1979) 297

16) H. Stöcker, R.Y. Cusson, J. Maruhn, and W. Greiner, Z. Phys. A294 (1980) 125 and Phys. Lett. 101B (1981) 379

17) H. Stöcker, M. Gyulassy and J. Boguta, Phys. Lett. 103B (1981) 269

18) J.P. Bondorf, Proceeding of the Topical Conf. on "Large Amplitude Collective Nuclear Motions", Lake Balaton, 1979, p. 482

19) K.K. Gudima and V.D. Toneev, Phys. Lett. 73B (1978) 293 and to be published

20) J. Cugnon, Phys. Rev. C22 (1980) 1885; J. Cugnon, J. Kinet, J. Vandermeulen, Nucl. Phys. A379 (1982) 553; and J. Cugnon, T. Mizutani, J. Vermeulen, Nucl. Phys. A352 (1981) 1807

21) G.F. Bertsch and J. Cugnon, Phys. Rev. C24 (1981) 2514

22) A. Mekjian, Phys. Rev. Lett. 38 (1977) 640; Phys. Rev. C17 (1978) 1051; and Nucl. Phys. A312 (1978) 451

23) P.J. Siemens, J.I, Kapusta, Phys. Rev. Lett. 43 (1979) 1486; J.I. Kapusta, D. Stottman, Phys. Rev. C23 (1981) 1282

24) S. Nagamiya, Phys. Rev. Lett. 49 (1982) 1383; S. Nagamiya, M.C. Lemaire, E. Moeller, S. Schnetzer, G. Shapiro, H. Steiner, I. Tannihata, Phys. Rev. C24 (1981) 971

25) H. Stöcker, Lawrence Berkeley Laboratory report 12302; see also ref. 7, p. 209

26) H. Stöcker, A.A. Ogloblin, and W. Greiner, Z. Physik A303 (1981) 259
27) J. Gosset, J.I. Kapusta, and G.D. Westfall, Phys. Rev. C18 (1978) 844; see also refs. 61-65 for classical statistics approaches
28) P.R. Subramanian, L.P. Csernai, H. Stöcker, J.A. Maruhn, W. Greiner, and H. Kruse, J. of Phys. G7 (1981) L241
29) H. Stöcker, to be published
30) M. Gyulassy, Nucl. Phys. A335 (1981) 395; J.R. Nix, Prog. Part. Nucl. Phys. 2 (1979) 237
31) H. Stöcker, J.A. Maruhn, and W. Greiner, Phys. Rev. Lett. 44 (1980) 725; Z. Phys. A293 (1979) 173
32) H. Stöcker, J. Hofmann, J.A. Maruhn, W. Greiner, Prog. Part. Nucl. Phys. 4 (1980) 133; Proc. Erice School on Heavy Ion Interactions at High Energies, Erice, Italy, 1979
33) A. Sandoval, R. Stock, H.E. Stelzer, R.E. Renfordt, J.W. Harris, J.P. Brannigan, J.V. Geaga, L.J. Rosenberg, L.S. Schroeder, K.L. Wolf, Phys. Rev. Lett. 45 (1980) 874; S.Y. Fung, W. Gorn, G.P. Kiernan, F.F. Liu, J.J. Lu, Y.T. Oh, J. Ozawa, R.T. Poe, L. Schroeder, H. Steiner, Phys. Rev. Lett. 40 (1978) 292
34) A.I. Warwick, H.H. Wieman H.H. Gutbrod, M.R. Maier, J. Péter, H.G. Ritter, H. Stelzer, F. Weik, M. Freedman, D.J. Henderson, S.B. Kaufman, E.P. Steinberg, B.D. Wilkins, Lawrence Berkeley Laboratory report 14015 (1982); and H.H. Gutbrod, A.I. Warwick, H.H. Wieman, Nucl. Phys. A387 (1982) 177
35) G. Buchwald, G. Graebner, J. Theis, J.A. Maruhn, W. Greiner, and H. Stöcker, to be published
36) H. Stöcker, L.P. Csernai, G. Graebner, G. Buchwald, H. Kruse, R.Y. Cusson, J.A. Maruhn, W. Greiner, Phys. Rev. C25 (1982) 1873; and H. Stöcker, C. Riedel, Y. Yariv, L.P. Csernai, G. Buchwald, G. Graebner, J.A. Maruhn, W. Greiner, K. Fraenkel, M. Gyulassy, B. Schürmann, G. Westfall, J.D. Stevenson, J.R. Nix, and D. Strottman, Phys. Rev. Lett. 47 (1981) 1807
37a) G. Buchwald, L.P. Csernai, J. Maruhn, W. Greiner, and H. Stöcker, Phys. Rev. C24 (1981) 135;
37b) L.P. Csernai, W. Greiner, H. Stöcker, I. Tanihata, S. Nagamiya, and J. Knoll, Phys. Rev. C25 (1982) 2482
38) R.M. DeVries, J.C. Peng, Phys. Rev. Lett. 43 (1979) 1373
39) W.A. Küppers, G. Wegmann, E.R. Hilf, Ann. Phys. 88 (1974) 454; S.A. Chin, J.D. Walecka, Phys. Lett. 52B (1974) 24; D.Q. Lamb, J.M. Lattimer, C. Pethick, D.G. Ravenhall, Phys. Rev. Lett. 41 (1978) 1623; M. Barranco, J.R. Buchler, Phys. Rev. C22 (1980) 1729; and B. Friedman, V.R. Pandharipande, Nucl. Phys. A361 (1981) 502
40) P. Danielewicz, Nucl. Phys. A314 (1979) 465
41) G. Röpke, L. Münchow, H. Schulz, Nucl. Phys. A379 (1982) 536, Phys. Lett. B110 (1982) 21; M. Curtin, H. Toki, and D.K. Scott, Michigan State University preprint (1981); D.K. Scott, invited talk at the XXth Intl. winter meeting on nuclear physics, Bormio, Italy, Jan. 1982
42) H. Jaqaman, A.Z. Mekjian, and L. Zamick, to be published; A. Mekjian, private communication
43) H.H. Gutbrod, H. Löhner, A.M. Poskanzer, T. Renner, H. Riedesel, H.G. Ritter, A. Warwick, F. Weik, and H. Wieman, Lawrence Berkeley Laboratory report 14888
44) M.E. Fisher, Physics 3 (1967) 255; J. Frenkel, in Kinetic Theory of Liquids (Oxford University Press, 1946); see also ref. 45, where these ideas have first been applied to high energy proton-nucleus interactions

45) R.W. Minich, S. Agarwal, A. Bujak, J. Chuang, J.E. Finn, L.J. Gutay, A.S. Hirsch, N.T. Porile, R.P. Scharenberg, B.C. Stringfellow, F. Turkot, Phys. Lett., 118B (1982) 458
J.E. Finn, et al., Phys. Rev. Lett., 49 (1982) 1321
46) G.F. Bertsch and P.J. Siemens, to be published
47) W. Benenson, G. Bertsch, G.M. Crawley, E. Kashy, J.A. Nolen, H. Bowman, J.G. Ingersoll, J.O. Rasmussen, J. Sullivan, M. Koike, M. Sasao, J. Peter, T.E. Ward, Phys. Rev. Lett. 43 (1979) 683 and 44 (1980) 54 (E);
J.P. Sullivan, et al., Phys. Rev. C25 (1982) 1499;
W. Benenson, Proc. Xth Intl. Workshop of Gross Properties of Nuclei and Nuclear Excitations, Hirschegg, Austria (1982) p. 85;
Y. Le Bornec, L. Bimbot, N. Koori, F. Reide, A. Willis, N. Willis, C. Wilkin, Phys. Rev. Lett. 47 (1981) 1870;
T. Johansson, H.A. Gustafsson, B. Jakobsson, P. Kristiansson, B. Noren, A. Oskarsson, L. Carlen, I. Otterlund, H. Ryde, J. Julien, C. Guet, R. Bertholet, M. Maurel, H. Nifenecker, P. Perrin, F. Schussler, G. Tibell, M. Buenerd, J.M. Loiseaux, P. Martin, J.P. Bondorf, O.B. Nielsen, A.O.T. Karvinen, J. Mougey, Phys. Rev. Lett. 48 (1982) 732;
J. Mougey, Nucl. Phys. A387 (1982) 109c;
J. Julien, Proc. 3rd Intl. Conf. Nuclear Reaction Mech., Varenna, Italy, June 1982;
B. Jakobsson, Proc. Nordic Meeting on Nuclear Physics, Fuglsø, Denmark, August 1982 (to be published in Phys. Skripta);
E. Grosse, et al., private communication and to be published
48) R. Stock. R. Bock, R. Brockmann, A. Dacal, J.W. Harris, M. Maier, M.E. Ortiz, H.G. Pugh, R.E. Renfordt, A. Sandoval, L.S. Schroeder, H. Stroebele, Phys. Rev. Lett. 49 (1982) 1236
49) R. Stock, H.H. Gutbrod, W.G. Meyer, A.M. Poskanzer, A. Sandoval, J. Gosset, C.H. King. G. King, Ch. Lukner, Nguyen Van Sen, G. D. Westfall, and K.L. Wolf, Phys. Rev. Lett. 44 (1980) 1243
50) H.G. Baumgardt, J.U. Schott, Y. Sakamoto, E. Schopper, H. Stöcker, J. Hofmann, W. Scheid, W. Greiner, Z. Phys. A273 (1975) 359; and J. Hofmann, H. Stöcker, U. Heinz, W. Scheid, and W. Greiner, Phys. Rev. Lett. 36 (1976) 88; and H.G. Baumgardt, and E. Schopper, J. Phys. Lett. G5 (1979) L231
51) J.I. Kapusta, D. Strottman, Phys. Lett. 103B (1981) 269
52) J. Cugnon, J. Knoll, C. Riedel, and Y. Yariv, Phys. Lett. 109B (1982) 167
53) M. Gyulassy, K.A. Fraenkel, H. Stöcker, Phys. Lett. 110B (1982) 185
54) H. Stöcker, G. Buchwald, L.P. Csernai, G. Graebner, J.A. Maruhn, and W. Greiner, Nucl. Phys. A387 (1982) 205c and to be published
55) G. Bertsch and A.A. Amsden, Phys. Rev. C18 (1978) 1293
56) H. Stöcker and B. Müller, Z. Naturforschung, in print
57) A. Huie, D. Beavis, S.Y. Fung, W. Gorn, D. Keane, J.J. Lu, R.T. Poe, B.C. Shen, and G. VanDalen, University of California at Riverside preprint; Phys. Rev. C, 27 (1983) 439
58) H. Stroebele, R. Brockmann, J.W. Harris, F. Riess, A. Sandoval, R. Stock, K.L. Wolf, H.G. Pugh, L.S. Schroeder, R.E. Renfordt, K. Tittel, and M. Maier, GSI preprint 1982-32, submitted to Phys. Rev. Lett.
59) D. Beavis, S.Y. Chu, S.Y. Fung, W. Gorn, A. Huie, D. Keane, J.J. Lu, R.T. Poe, B.C. Shen, G. VanDalen, Univ. of California at Riverside preprint, submitted to Phys. Rev. Lett.

60) H.H. Gutbrod, H. Löhner, A.M. Poskanzer, T. Renner, H. Riedesel, H.G. Ritter, A. Warwick, F. Weik, H. Weiman, Lawrence Berkeley Laboratory preprint 14980 (1982), submitted to Phys. Rev. Lett.
61) P. Bond, P.I. Johansen, S.E. Koonin, and S. Garpman, Phys. Lett. 71B (1977) 43
62) J. Randrup and S.E. Koonin, Nucl. Phys. A356 (1981) 223
63) G. Fai and J. Randrup, Nucl. Phys. A381 (1982) 537
64) T.S. Biro, H.W. Barz, B. Lukacs, J. Zimanyi, Phys. Rev. C in print
65) J. Bondorf, I.N. Mishustin, C. Pethick, to be published; and J. Bondorf, Nucl. Phys. A387 (1982) 25c
66) J. Boguta and H. Stöcker, Phys. Lett. 120B (1983) 289